Rotational Dynamics

DOI: 10.1002/ange.201306193

Modulating the Rotation of a Molecular Rotor through Hydrogen-Bonding Interactions between the Rotator and Stator**

Qian-Chong Zhang, Fang-Ting Wu, Hui-Min Hao, Hang Xu, Hai-Xia Zhao, La-Sheng Long,* Rong-Bin Huang, and Lan-Sun Zheng*

Dedicated to Professor Xiao-Zeng You on the occasion of his 80th Birthday

Molecular rotors have attracted attention because of their potential applications in the fields of ferroelectric,[1–3] conductive,[4–5] and dielectrophoresis materials and in optical molecular devices.[6–9] The molecular rotors synthesized thus far can primarily be divided into two types: mono-component molecular rotors and multiple-component molecular rotors. In the former, the stator and rotator are contained within the same molecule,[10–15] whereas, in the latter, the stator and rotator are contained in different molecules.[16–20] Although the components and structures of molecular rotors differ, their physical properties primarily depend on the rotational dynamics of the rotators.[4,8] Therefore, modulating the rotational rate of the rotator is critical to the application of molecular rotors.

In the effort to modulate the rotational rate of molecular rotors, chemists have demonstrated that the rotational rate of the rotator in a mono-component molecular rotor can be controlled by chemically modifying its stator. However, the ability to modulate the scale of the energy barrier with respect to the rotation of the rotator is limited, because of the interaction between the stator and rotator, which primarily consists of van der Waals forces,[15] not hydrogen-bonding interactions. In comparison, modulating the rotational rate of a rotator in a multiple-component molecular rotor through hydrogen-bonding interactions between the rotator and stator is relatively simple.[4] However, not only does the construction of multiple-component molecular rotors require the precise incorporation of all components, but the large-amplitude molecular rotations within the close-packed crystals often result in the melting or decomposition of such crystals.[1] Thus, modulating the rotational rate of a rotator in the solid state through hydrogen-bonding interactions between the rotator and stator remains a formidable challenge. Here we report the syntheses and crystal structures of two molecular rotors: 1,1′-(2-fluoro-1,4-phenylene)bis(3-phenethyl-5-phenylpent-1-yn-3-ol) (FPBP, **1a**) and 1,1′-(2-amino-1,4-phenylene)bis(3-phenethyl-5-phenylpent-1-yn-3-ol) (APBP, **1b**). Our investigation of the rotator rotation through the imaginary parts of the complex dielectric constant (ε'') of each molecular rotor at various frequencies and temperatures reveals that the rotation of the mono-component molecular rotor can be modulated through hydrogen-bonding interactions between the rotator and stator. More importantly, the hydrogen-bonding interactions between the rotator and stator can significantly enhance the energy barrier to the rotation of the molecular rotor.

Compounds **1a** and **1b** were prepared according to Scheme 1. Compounds **2** and **3** were synthesized according to methods previously reported in the literature.[21] The treatment of **3** with trimethylsilylethynylmagnesium bromide generated compound **4**. The reaction of **4** with potassium carbonate yielded compound **5**. Compounds **1a** and **1b** were synthesized using the Sonogashira coupling[22] of **5** with 1,4-dibromo-2-fluorobenzene and 2,5-dibromoaniline with total yields of 57.5% and 48.1%, respectively (see section S1 in the Supporting Information).

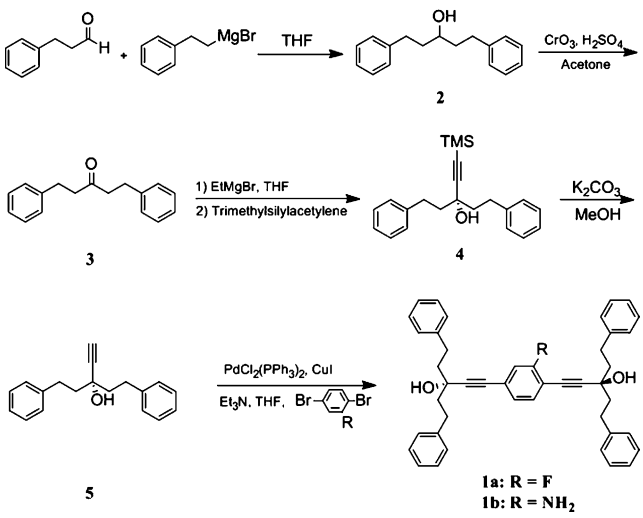

Scheme 1. Synthetic route for compounds **1a** and **1b**.

Single-crystal structural analysis at 273(2) K revealed that **1a** crystallizes in the noncentrosymmetric space group $Pca2_1$. The asymmetrical unit in **1a** consists of one dumbbell-shaped FPBP molecule that contains the stator and hydroxy groups in

[*] Q.-C. Zhang, F.-T. Wu, H.-M. Hao, H. Xu, H.-X. Zhao, Prof. Dr. L.-S. Long, Prof. R.-B. Huang, Prof. Dr. L.-S. Zheng
State Key Laboratory of Physical Chemistry of Solid Surfaces and the Department of Chemistry, College of Chemistry and Chemical Engineering, Xiamen University
Xiamen 361005 (China)
E-mail: lslong@xmu.edu.cn
hxzhao@xmu.edu.cn

[**] This work was supported by the 973 project from MSTC (grant number 2012CB821704) and The NNSFC (grant numbers 20825103, 90922031, 21001089, and 21021061).

Supporting information for this article is available on the WWW under http://dx.doi.org/10.1002/anie.201306193.

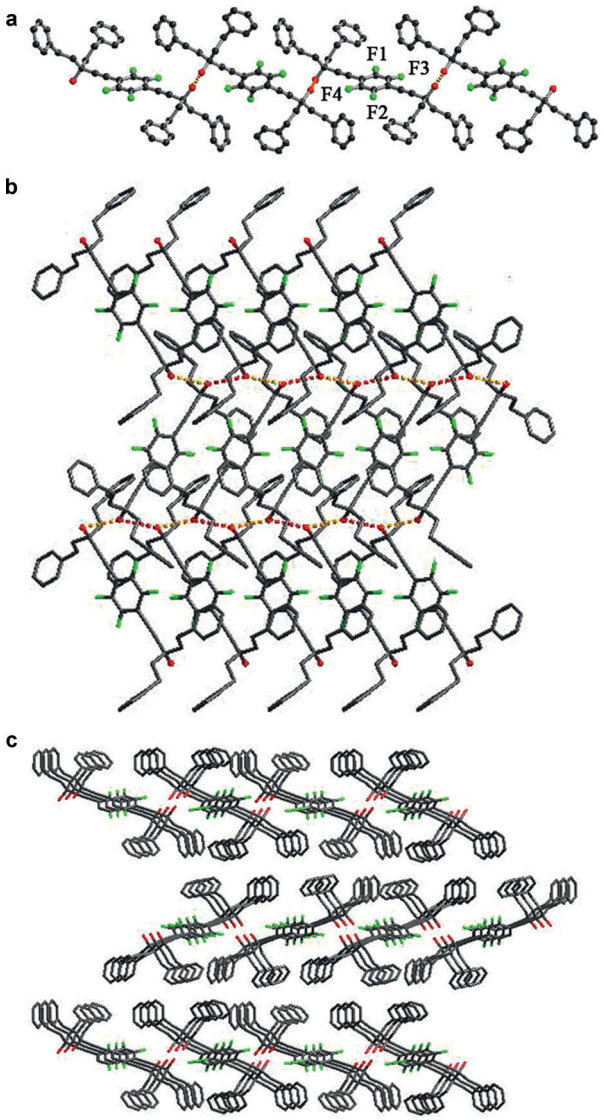

Figure 1. a) The 1D chain structure in **1a**; b) the 2D layer structure in **1a**; c) the 3D structure of **1a**. The hydrogen atoms are omitted for clarity.

a *trans* configuration. The two adjacent molecules in **1a** that are connected through hydrogen-bonding interactions between two hydroxy groups (O-H···O = 3.081(2) Å, H···O = 2.27 Å, ∡O-H···O = 160.3°) from two FPBP molecules in a head-to-tail arrangement generate a 1D chain structure (Figure 1a). Connection of the adjacent 1D chains through hydrogen-bonding interaction between the adjacent hydroxy groups (O-H···O = 3.178(2) Å, H···O = 2.44 Å, ∡O-H···O = 145.4°) respectively from the two adjacent chains forms a 2D layer structure (Figure 1b). Extending the 2D layer structure leads to a 3D structure of **1a** through both hydrogen-bonding interactions between the hydroxy groups of one layer and the F atom of the adjacent layers (O-H···F = 3.337(9) Å, H···F = 2.53 Å, ∡O-H···F = 159.5°)[23] and van der Waals interactions (Figure 1c).

Although the phenyl ring of arylene in **1a** contains one fluorine atom, fluorine atoms occupy four different positions on the phenyl ring based on the different Fourier maps. Moreover, the occupancies of fluorine atoms at the four positions differ, implying that the phenyl ring of arylene in **1a** may rotate rapidly.

To confirm the rotation of the rotator in **1a**, we measured the imaginary parts of its complex dielectric constant (ε'') at various frequencies and temperatures based on the pellet of **1a**. As shown in Figure 2, at $f = 10^{3.5}$ Hz, ε'' was almost

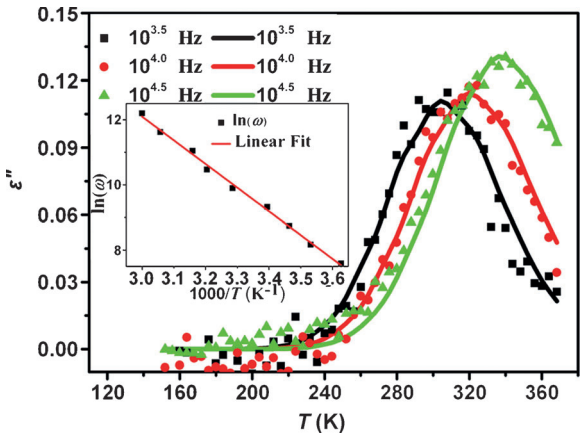

Figure 2. The plot of ε'' versus temperature for **1a**. The dots represent the experimental data, and the lines represent the simulated data calculated from Equations (2) and (3). The inset provides the linear fitting of $\ln(\omega)$ versus $1/T_{peak}$.

constant between 150 and 220 K. At temperatures above 220 K, the ε'' values increased with increasing temperature and reached a maximum at approximately 304 K; the ε'' values then decreased with further increases in temperature. In addition to the temperature, the frequency significantly influenced the ε'' values of **1a**. At $f = 10^4$ Hz, the ε'' maximum appeared at approximately 317 K, whereas the ε'' maximum shifted to approximately 333 K at $f = 10^{4.5}$ Hz (the full experiment data for ε'' from $10^{2.5}$ Hz to $10^{4.5}$ Hz are provided in section S3 in the Supporting Information). The imaginary parts of the complex dielectric constant (ε'') at various frequencies and temperatures indicate that **1a** undergoes the Debye-type single relaxation process.[19]

Based on the Debye-type single relaxation process, the relationship of ε'' and temperature (T) in Equation (1),

$$\varepsilon''(T) = \frac{\omega\tau(T)}{1+\omega^2\tau(T)^2} \quad (1)$$

where ω is the angular frequency of the test field and $\tau(T)$ is the relaxation time, which is a function of the temperature in accordance with Equation (2),

$$\frac{1}{\tau} = \omega_0 \exp\left(\frac{-E_a}{k_B T}\right) \quad (2)$$

reaches a maximum when $\omega\tau(T) = 1$. Thus, the test frequency can be used to estimate the rotational rate ($1/\tau$) at the temperature where ε'' is maximized. Because the rotational

rate ($1/\tau$) can be expressed as Equation (2), where E_a is the activation energy, ω_0 is a pre-exponential factor, and k_B is the Boltzmann constant, an ω_0 value of $5.3\times10^{14}\ s^{-1}$, and an E_a of 14.4 kcal mol^{-1} were obtained from the plot of $1/T_{peak}$ versus $\ln(\omega)$ (Figure 2, inset).

Given the relationship between ε'' and T in Equation (1) obtained under the assumption that all the rotators rotate at the same frequency (i.e., that the thermodynamic rotation is a statistical result[24]), a distribution factor $G(\tau)$ can be introduced into Equation (1) to describe the distribution of the rotational frequencies.[19,25] According to the time/temperature superposition principle and Equation (2), the distribution factor $G(\tau)$ can be transformed into a Gaussian-type energy function, $G(E_a)$.[25–27] Therefore, the simulated curves for the test frequency can be plotted according to Equation (3)

$$\varepsilon''(T)=\int_0^\infty G(\tau)\frac{\omega\tau(T)}{1+\omega^2\tau(T)^2}d\tau \qquad (3)$$

using multiple energy barriers that range from 9.8 kcal mol^{-1} to 18.8 kcal mol^{-1} at 1.0 kcal mol^{-1} intervals (Figure 2).[28] As indicated in Figure 2, the simulated curve for each test frequency matches the experimental data.

The E_a value for **1a** (14.4 kcal mol^{-1}) is significantly larger than that for 1,4-bis[tri-(*meta*-methoxyphenyl)propynylbenzene (11.7 kcal mol^{-1})[15] although the packing coefficient of **1a** (0.72) is smaller than that of 1,4-bis[tri-(*meta*-methoxyphenyl)propynylbenzene (0.73).[29] Because a larger packing coefficient often results in a larger E_a value for the rotation of a molecular rotor,[15] one can attribute the E_a in **1a**, which is larger than that in 1,4-bis[tri-(*meta*-methoxyphenyl)propynylbenzene, to the hydrogen-bonding interaction between the rotator (fluorine atom) and stator (hydroxy group) in **1a**.

To determine how the hydrogen-bonding interactions between the rotator and stator enhance the E_a in **1a**, the crystal structures of a single **1a** crystal were measured at 123(2), 213(2), 273(2), and 313(2) K (see section S2 in the Supporting Information). These measurements indicate that the occupancy of the fluorine atom at position F4 in **1a** decreases as temperature decreases. At and below 213 K, the occupancy of the fluorine atom at position F4 becomes zero, leaving three disordered F atoms (F1, F2, and F3) on the phenyl ring. A further investigation of the crystal structures at different temperatures revealed that the strength of the hydrogen-bonding interaction (F3···O1)[23] between the adjacent FPBP molecules in **1a** increases with a decrease in temperature (Table 1).

Thus, the fluorine atom at the F4 position could be only detected at higher temperatures because higher temperatures not only favor the rotation of the rotator, but also weaken the hydrogen-bonding interaction (F3···O1) between the rotator and stator in **1**, which, in turn, decreases the rotational friction. Thus, the disorder of the fluorine atom in the rotator increases with increasing temperature. The disappearance of the fluorine atom from the F4 position in the rotator at lower temperatures is unambiguously related to the formation hydrogen bonds (F3···O1) between the rotator and stator in **1a**, which prevents the fluorine atom at the F3 position from becoming disordered or rotating. This deduction is consistent with the occupancy of the fluorine atom at the F1 position, which approaches that of the fluorine atom at the F2 position at higher temperatures, and with the occupancy of the fluorine atom at the F1 position, which diverges from that of the fluorine atom at the F2 position at lower temperatures (see section S2 in the Supporting Information).

Table 1: Hydrogen-bonding interaction of F3···O1 in **1a** at various temperatures.

T [K]	F3···O1 [Å]	F3···HO1 [Å]	∡ F3···H–O1
123(2)	3.278(5)	2.47	155.4°
213(2)	3.303(8)	2.49	159.4°
273(2)	3.337(9)	2.53	159.5°
313(2)	3.333(9)	2.57	154.4°

To further confirm that the hydrogen-bonding interactions between the rotator and stator are important in enhancing the E_a in **1a**, the molecular rotor **1b** was synthesized with the fluorine atom replaced by an amino group. Single-crystal structural analysis revealed that **1b** crystallizes in space group $P\bar{1}$. Although the space group of **1b** differs from that of **1a**, the 1D chain in **1b** can also be viewed as the connection between adjacent APBP molecules through the hydrogen bonding of two hydroxy groups (O-H···O = 2.801(4) Å, H···O = 1.96 Å, ∡O-H···O = 168.2°) from two APBP molecules in a head-to-tail arrangement, similar to that in **1a** (Figure S2a). Moreover, the two compounds have similar packing models (Figure S2). However, the hydrogen-bonding interaction between the rotator (amino group) of one APBP molecule and the stator (hydroxy group) of an adjacent APBP molecule in **1b** (O-H···N = 2.881(15) Å, H···O = 2.13 Å, ∡O-H···O = 147.2°; Figure 3) is significantly stronger than that in **1a** (Figure 3a). Therefore, we expected that the

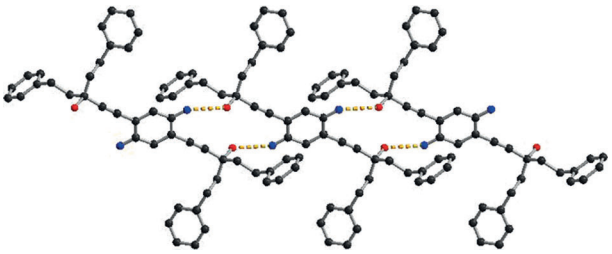

Figure 3. The hydrogen bonds between the hydroxy and amino groups. The hydrogen atoms are omitted for clarity.

E_a for the rotation of the rotator in **1b** would be significantly higher than that in **1a** if the hydrogen-bonding interaction between the rotator and stator are important in enhancing the E_a value for the rotation of the rotor.

In fact, measurements of the ε'' values at various frequencies and temperatures (Figure 4 and Figures S4 and S5 in which the rapid increase in ε'' at temperatures above 370 K is due to an increase in the conductivity at high temperatures) indicate that the maximum ε'' for **1b** occurs at a significantly higher temperature than that for **1a** at the same test frequency. For example, at $f=10^4$ Hz, the maximum ε'' for

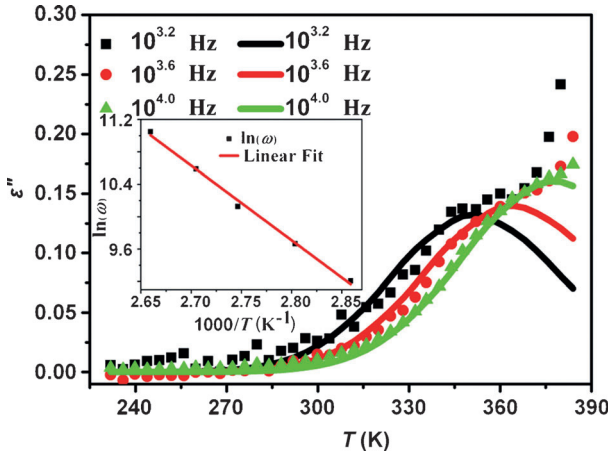

Figure 4. A plot of ε'' versus temperature for **1b**. The dots represent the experimental data, and the lines represent the simulated data calculated using Equations (2) and (3). The inset shows a linear fitting of $\ln(\omega)$ versus $1/T_{peak}$.

1b occurs at approximately 375 K, whereas that for **1a** occurs at approximately 320 K at the same frequency. Based on the date in Figure 4, the ω_0 and E_a values for **1b** are 5.7×10^{15} s^{-1} and 18.9 kcal mol^{-1}, respectively, which indicates that the hydrogen-bonding interaction between the rotator and stator can influence the E_a for the rotation of the molecular rotor.

In summary, we synthesized two molecular rotors, **1a** and **1b** and determined the activation energy for the rotations of **1a** and **1b.** We obtained an E_a value for **1a** of 14.4 kcal mol^{-1}, which is significantly lower than that for **1b** (18.9 kcal mol^{-1}). Single-crystal structural analysis revealed that the hydrogen-bonding interactions between the rotator and stator play a key role in determining the activation energy for the rotation. Compounds **1a** and **1b** represent the first examples of mono-component molecular rotors in which the rotator rotation has been regulated by hydrogen-bonding interactions between the rotator and stator. Thus, the present work may open a pathway to the regulation of rotator rotation in mono-component molecular rotors.

Received: July 17, 2013
Revised: August 19, 2013
Published online: October 2, 2013

Keywords: activation energies · hydrogen bonds · molecular rotors · rotational dynamics · structure elucidation

[1] T. Akutagawa, H. Koshinaka, D. Sato, S. Takeda, S. Noro, H. Takahashi, R. Kumai, Y. Tokura, T. Nakamura, *Nat. Mater.* **2009**, *8*, 342 – 347.
[2] D. W. Fu, W. Zhang, H. L. Cai, Y. Zhang, J. Z. Ge, R. G. Xiong, S. D. Huang, *J. Am. Chem. Soc.* **2011**, *133*, 12780 – 12786.
[3] Y. Zhang, W. Zhang, S. H. Li, Q. Ye, H. L. Cai, F. Deng, R. G. Xiong, S. D. Huang, *J. Am. Chem. Soc.* **2012**, *134*, 11044 – 11049.
[4] C. Lemouchi, C. Mézière, L. Zorina, S. Simonov, A. Rodríguez-Fortea, E. Canadell, P. Wzietek, P. Auban-Senzier, C. Pasquier, T. Giamarchi, M. A. Garcia-Garibay, P. Batail, *J. Am. Chem. Soc.* **2012**, *134*, 7880 – 7891.
[5] J. S. Seldenthuis, F. Prins, J. M. Thijssen, H. S. J. van der Zant, *ACS Nano* **2010**, *4*, 6681 – 6686.
[6] E. R. Kay, D. A. Leigh, F. Zerbetto, *Angew. Chem.* **2007**, *119*, 72 – 196; *Angew. Chem. Int. Ed.* **2007**, *46*, 72 – 191.
[7] M. G. L. van den Heuvel, M. P. de Graaff, C. Dekker, *Science* **2006**, *312*, 910 – 914.
[8] W. Setaka, K. Yamaguchi, *Proc. Natl. Acad. Sci. USA* **2012**, *109*, 9271 – 9275.
[9] C. Lemouchi, K. Iliopoulos, L. Zorina, S. Simonov, P. Wzietek, T. Cauchy, A. Rodríguez-Fortea, E. Canadell, J. Kaleta, J. Michl, D. Gindre, M. Chrysos, P. Batail, *J. Am. Chem. Soc.* **2013**, *135*, 9366 – 9376.
[10] Z. Dominguez, H. Dang, M. J. Strouse, M. A. Garcia-Garibay, *J. Am. Chem. Soc.* **2002**, *124*, 2398 – 2399.
[11] Z. Dominguez, T. V. Khuong, H. Dang, C. N. Sanrame, J. E. Nuñez, M. A. Garcia-Garibay, *J. Am. Chem. Soc.* **2003**, *125*, 8827 – 8837.
[12] B. Rodríguez-Molina, N. Farfán, M. Romero, J. M. Méndez-Stivalet, R. Santillan, M. A. Garcia-Garibay, *J. Am. Chem. Soc.* **2011**, *133*, 7280 – 7283.
[13] C. S. Vogelsberg, M. A. Garcia-Garibay, *Chem. Soc. Rev.* **2012**, *41*, 1892 – 1910.
[14] E. Escalante-Sánchez, B. Rodríguez-Molina, M. A. Garcia-Garibay, *J. Org. Chem.* **2012**, *77*, 7428 – 7434.
[15] Z. J. O'Brien, A. Natarajan, S. Khan, M. A. Garcia-Garibay, *Cryst. Growth Des.* **2011**, *11*, 2654 – 2659.
[16] H. Kitagawa, Y. Kobori, M. Yamanaka, K. Yoza, K. Kobayashi, *Proc. Natl. Acad. Sci. USA* **2009**, *106*, 10444 – 10448.
[17] L. Kobr, K. Zhao, Y. Q. Shen, A. Comotti, S. Bracco, R. K. Shoemaker, P. Sozzani, N. A. Clark, J. C. Price, C. T. Rogers, J. Michl, *J. Am. Chem. Soc.* **2012**, *134*, 10122 – 10131.
[18] S. L. Gould, D. Tranchemontagne, O. M. Yaghi, M. A. Garcia-Garibay, *J. Am. Chem. Soc.* **2008**, *130*, 3246 – 3247.
[19] S. Devautour-Vinot, G. Maurin, C. Serre, P. Horcajada, D. Paula da Cunha, V. Guillerm, E. de Souza Costa, F. Taulelle, C. Martineau, *Chem. Mater.* **2012**, *24*, 2168 – 2177.
[20] E. B. Winston, P. J. Lowell, J. Vacek, J. Chocholoušová, J. Michl, J. C. Price, *Phys. Chem. Chem. Phys.* **2008**, *10*, 5188 – 5191.
[21] H. Ueki, T. Chiba, T. Yamazaki, T. Kitazume, *J. Org. Chem.* **2004**, *69*, 7616 – 7627.
[22] K. Sonogashira, Y. Tohda, N. Hagihara, *Tetrahedron Lett.* **1975**, *16*, 4467 – 4470.
[23] K. Reichenbächer, H. I. Süss, J. Hulliger, *Chem. Soc. Rev.* **2005**, *34*, 22 – 30.
[24] A. Bokov, Z. G. Ye, *J. Adv. Dielectr.* **2012**, *2*, 1241010.
[25] S. Devautour, J. Vanderschuere, J. C. Giuntini, F. Henn, J. V. Zanchetta, *J. Appl. Phys.* **1997**, *82*, 5057 – 5062.
[26] A. Nicolas, S. Devautour-Vinot, G. Maurin, J. C. Giuntini, F. Henn, *J. Phys. Chem. C* **2007**, *111*, 4722 – 4726.
[27] F. Kremer, A. Schönhals, *Broadband dielectric spectroscopy*, Springer, Berlin, **2003**, pp. 10 – 20.
[28] R. D. Horansky, L. I. Clarke, J. C. Price, T. V. Khuong, P. D. Jarowski, M. A. Garcia-Garibay, *Phys. Rev. B* **2005**, *72*, 014302.
[29] A. Gavezzotti, *J. Am. Chem. Soc.* **1983**, *105*, 5220 – 5225.